

Electronic Supplementary Information

Halo-phenyl based linear dipodal receptors for entrapment of anions/anionic associations within neutral non-cooperative self- assemblies

Utsab Manna and Gopal Das *

Department of Chemistry, Indian Institute of Technology Guwahati,

Assam-781039, India

E-mail: gdas@iitg.ernet.in

Characterization of free receptors L_1 and L_2 :

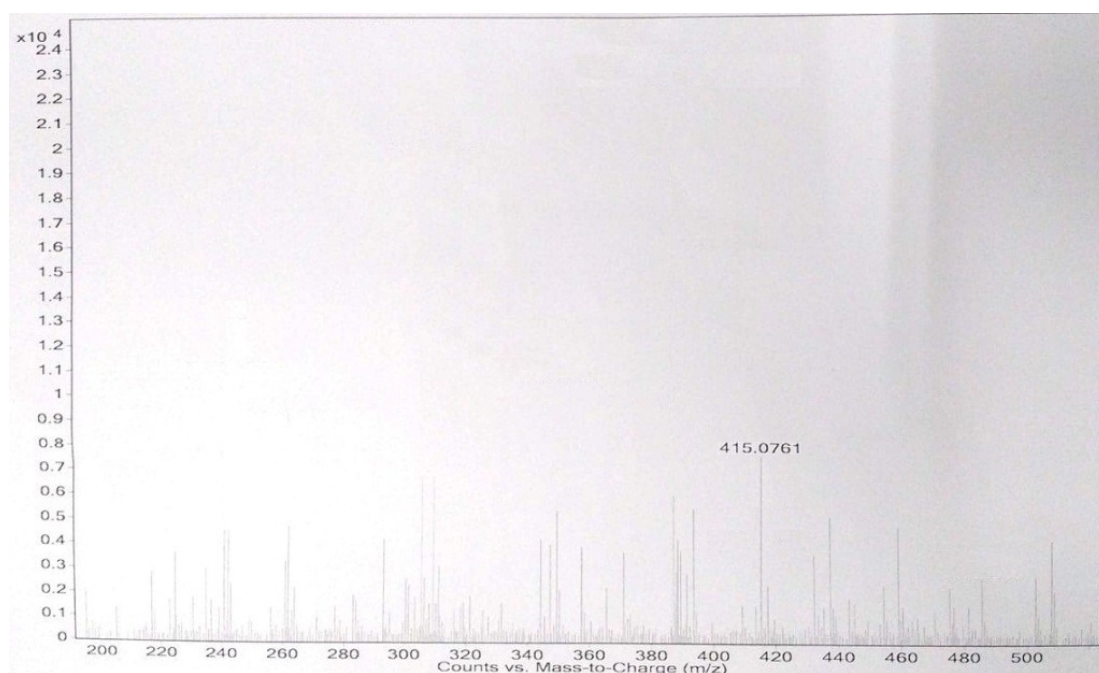


Figure S1: ESI-Mass spectrum of *para*-chlorophenyl functionalized *para*-phenylenediamine based bis-urea receptor L_1 .

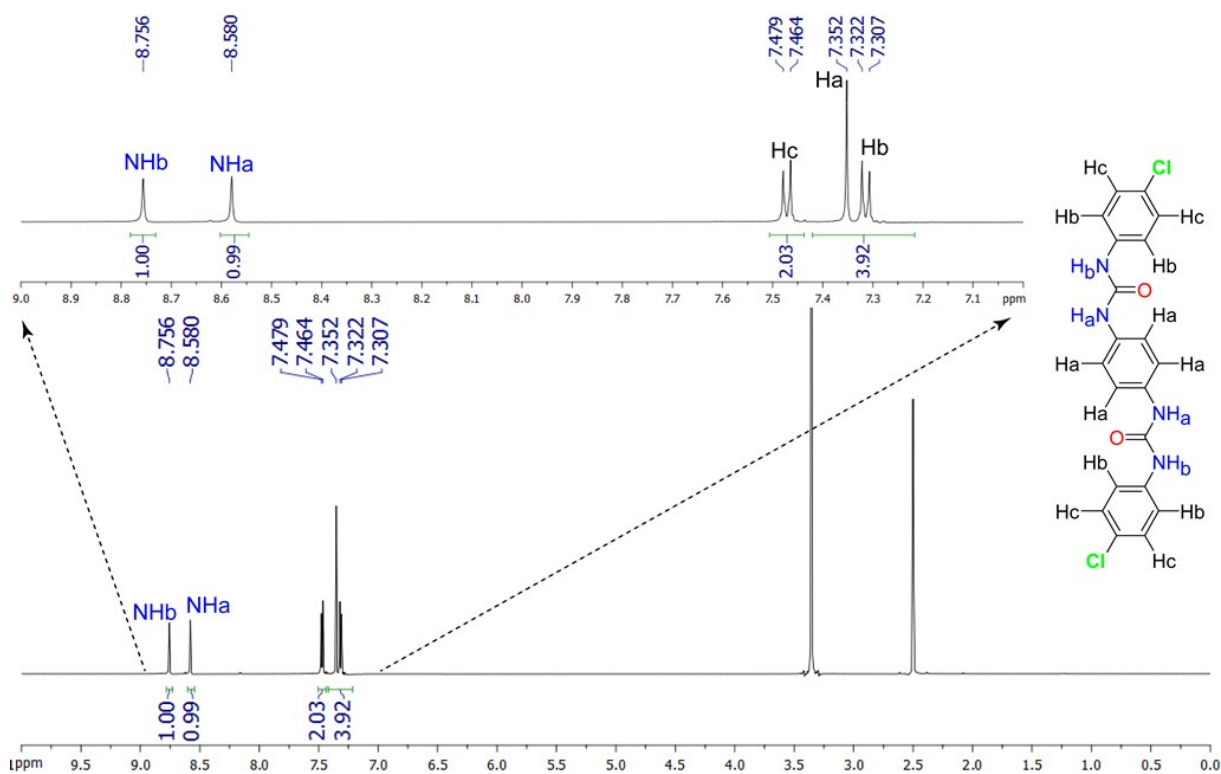


Figure S2: Integrated 1H -NMR spectrum (full as well as expanded) and interpretation of all hydrogen atoms of free dipodal bis-urea *para*-chloro isomer L_1 in $DMSO-d_6$ at $25^\circ C$.

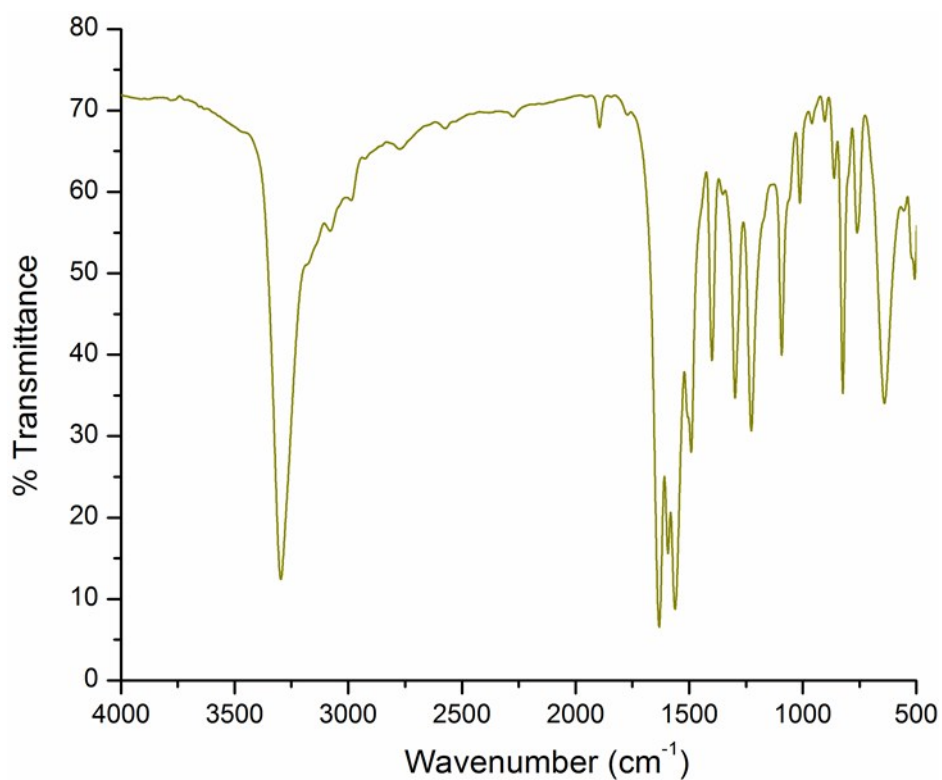


Figure S3: FT-IR spectrum of **L₁** recorded in KBr pellet.

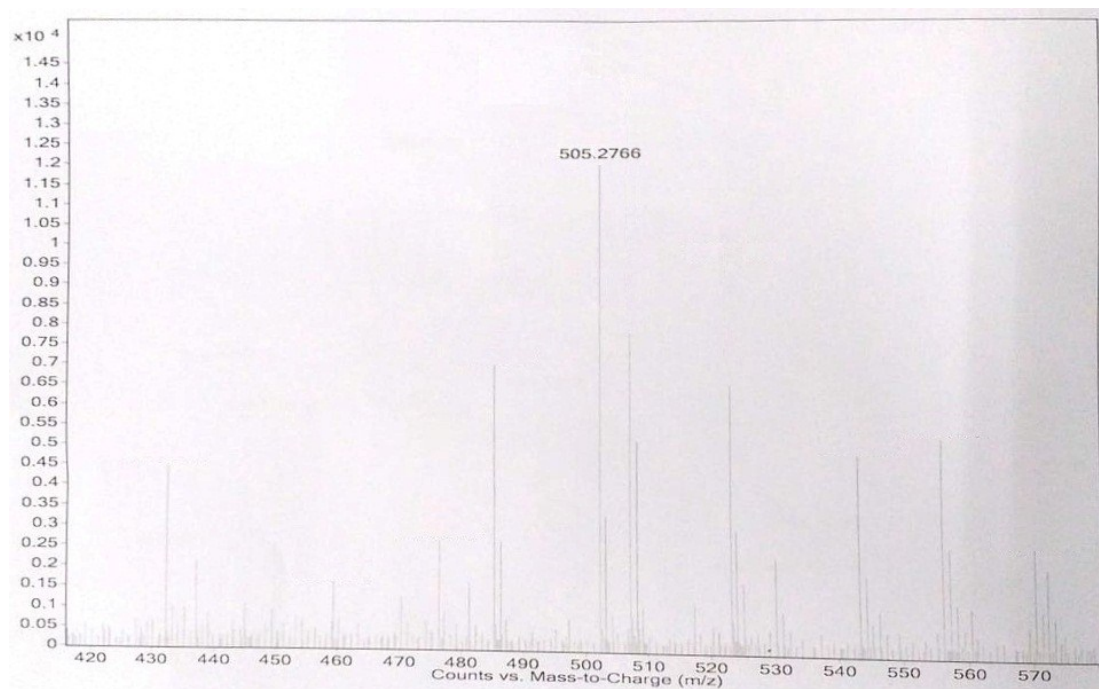


Figure S4: ESI-Mass spectrum of *para*-bromophenyl functionalized *para*-phenylenediamine based bis-urea receptor **L₂**.

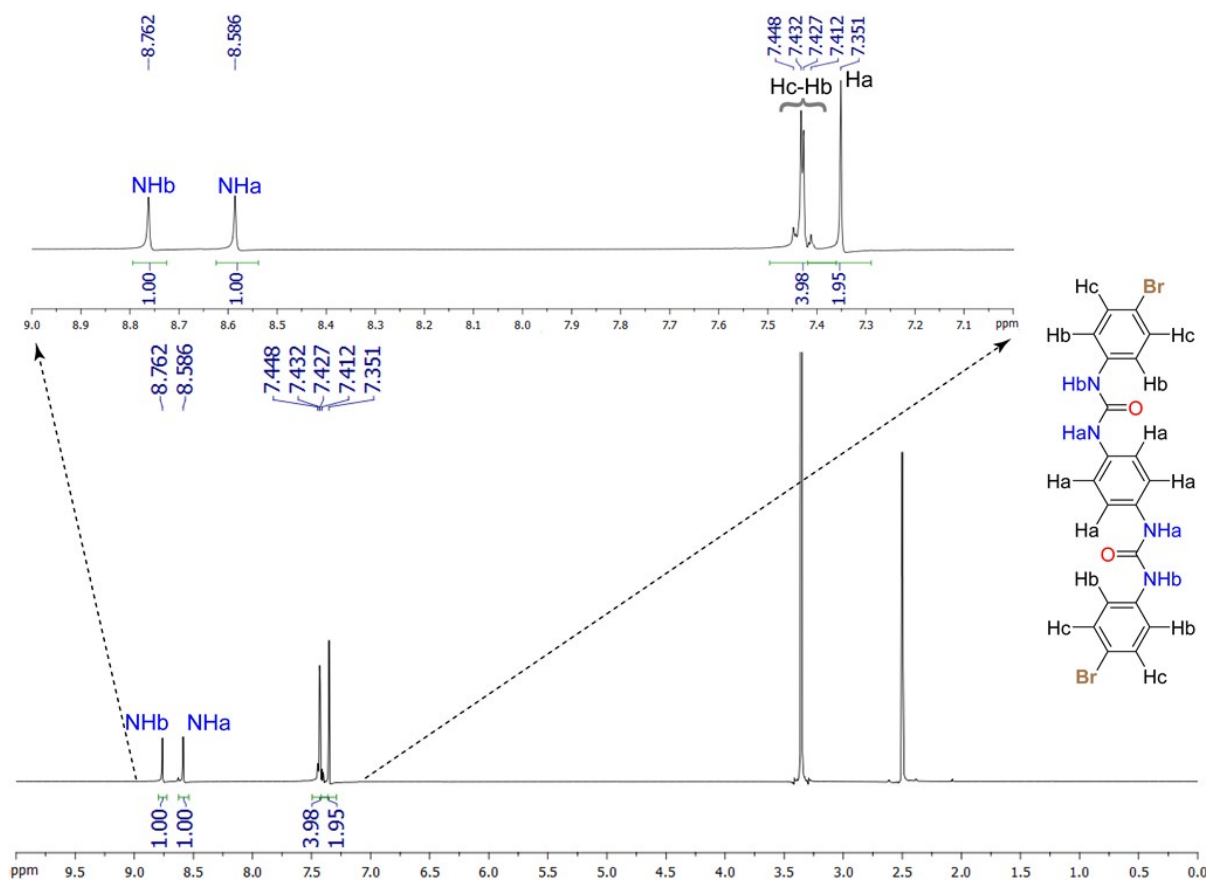


Figure S5: Integrated ^1H -NMR spectrum (full as well as expanded) and interpretation of all hydrogen atoms of free dipodal bis-urea *para*-bromoisomer L_2 in DMSO-d_6 at 25°C .

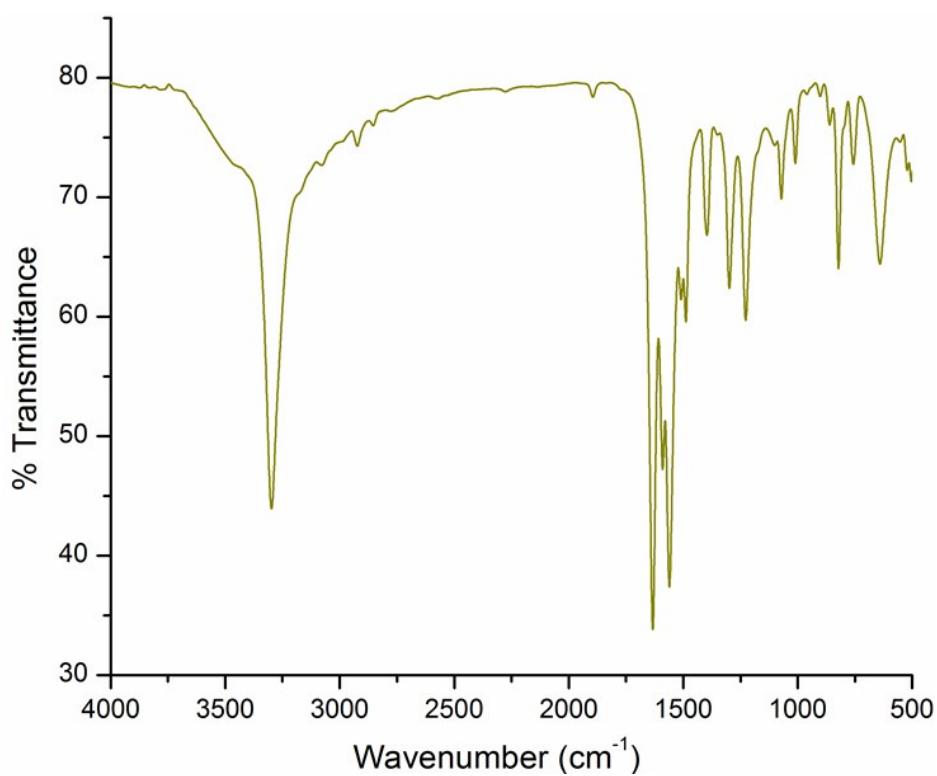


Figure S6: FT-IR spectrum of L_2 recorded in KBr pellet.

Characterization of neutral anion complexes of receptors:

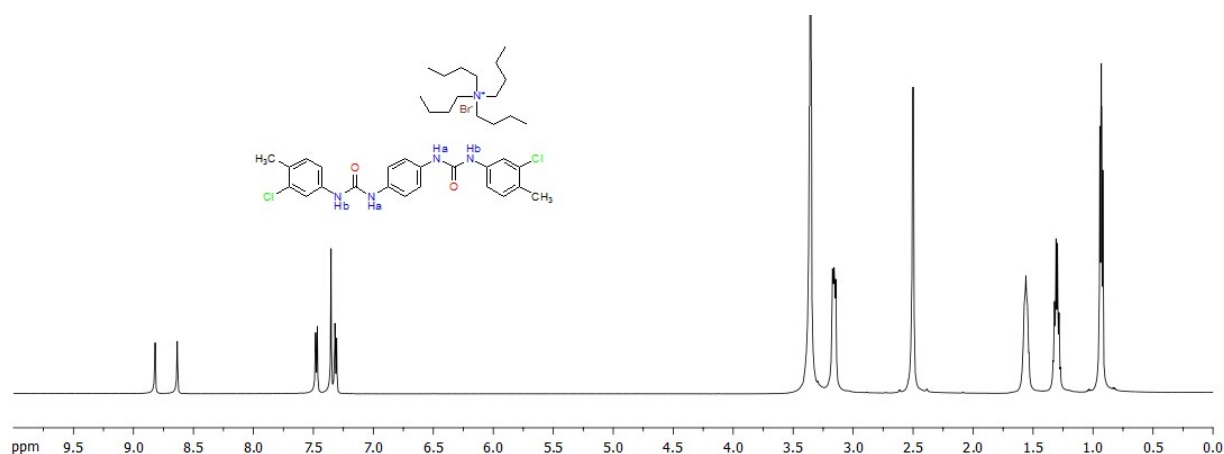


Figure S7: ^1H NMR full and expanded spectrum of bromide complex **1a** of **L₁** as recorded in $\text{DMSO-}d_6$ at 298 K.

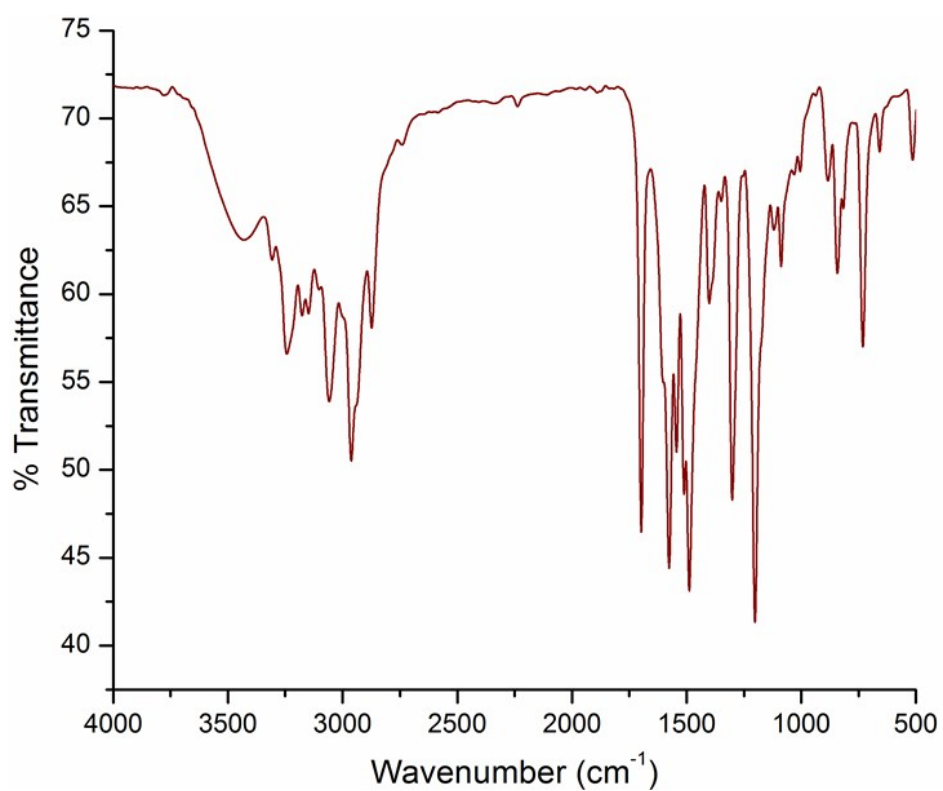


Figure S8: FT-IR spectrum of complex **1a** of **L₁** recorded in KBr pellet.

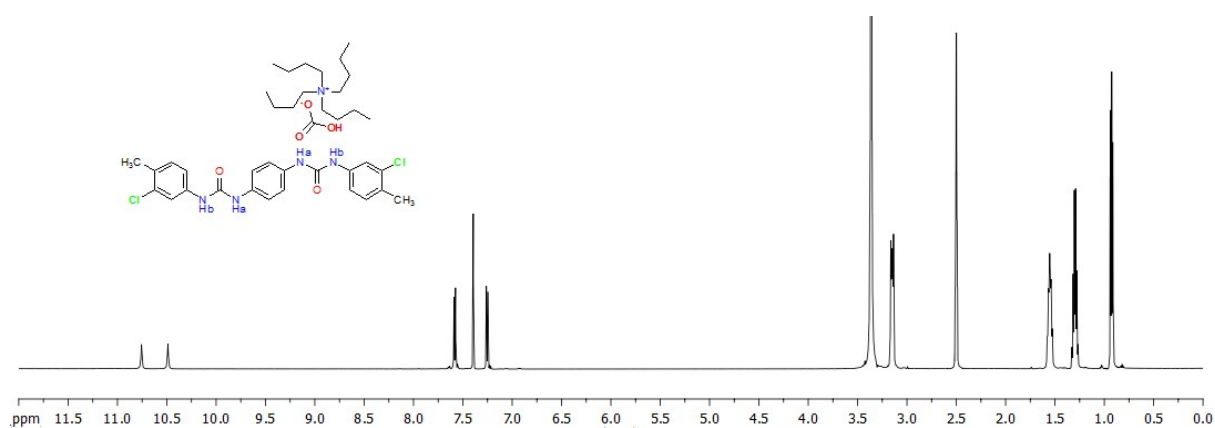


Figure S9: ^1H NMR full and expanded spectrum of hydroxide induced hydrogencarbonate dimer entrapped complex **1b** of **L₁** as recorded in $\text{DMSO-}d_6$ at 298 K.

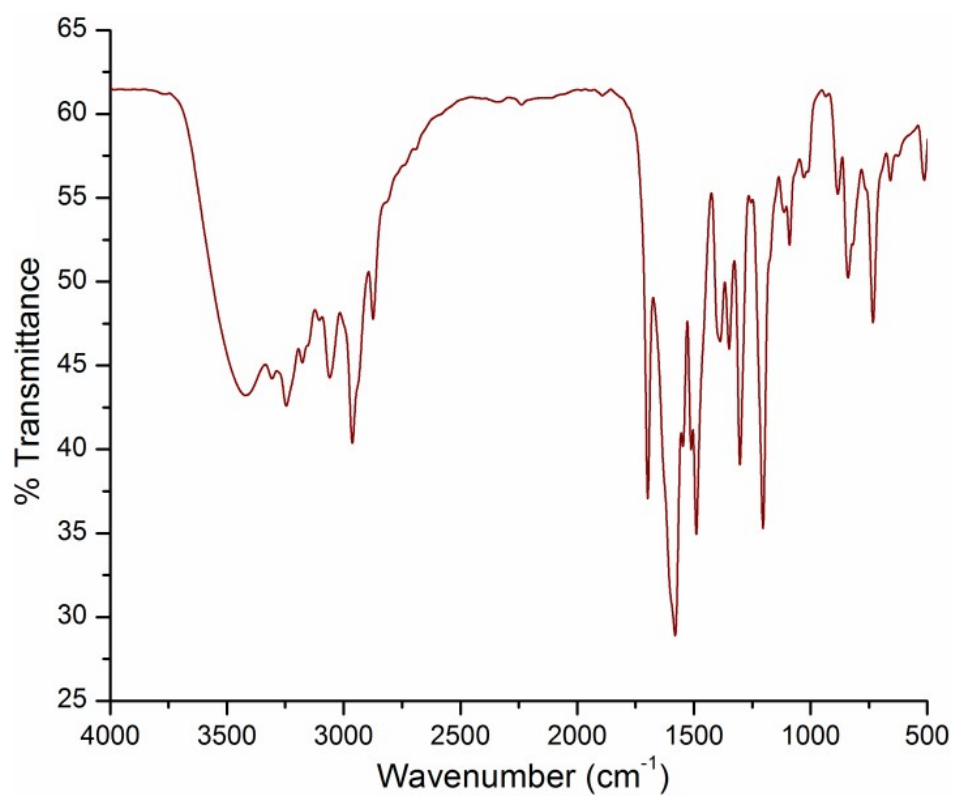


Figure S10: FT-IR spectrum of complex **1b** of **L₁** recorded in KBr pellet.

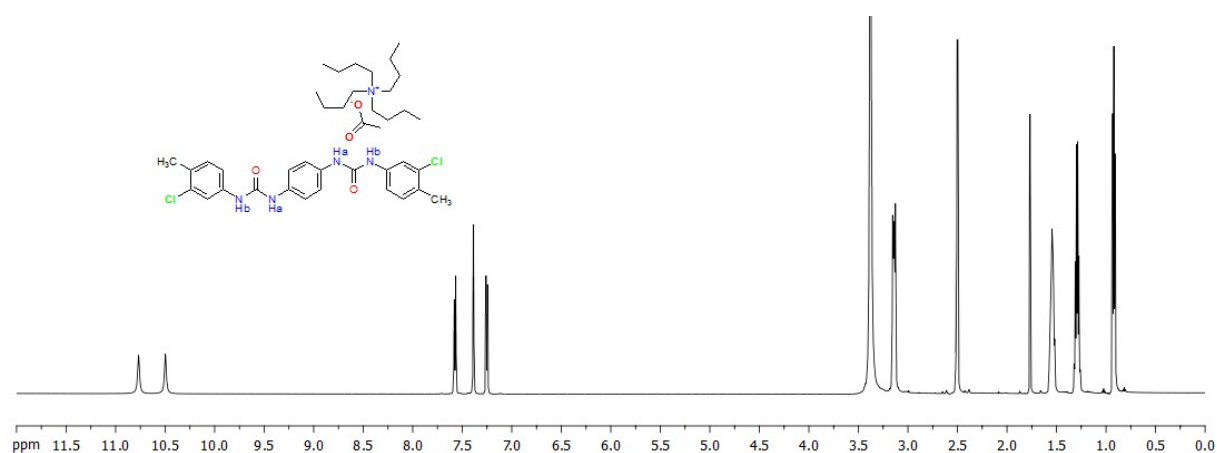


Figure S11: ^1H NMR full and expanded spectrum of acetate entrapped complex **1c** of **L₁** as recorded in $\text{DMSO-}d_6$ at 298 K.

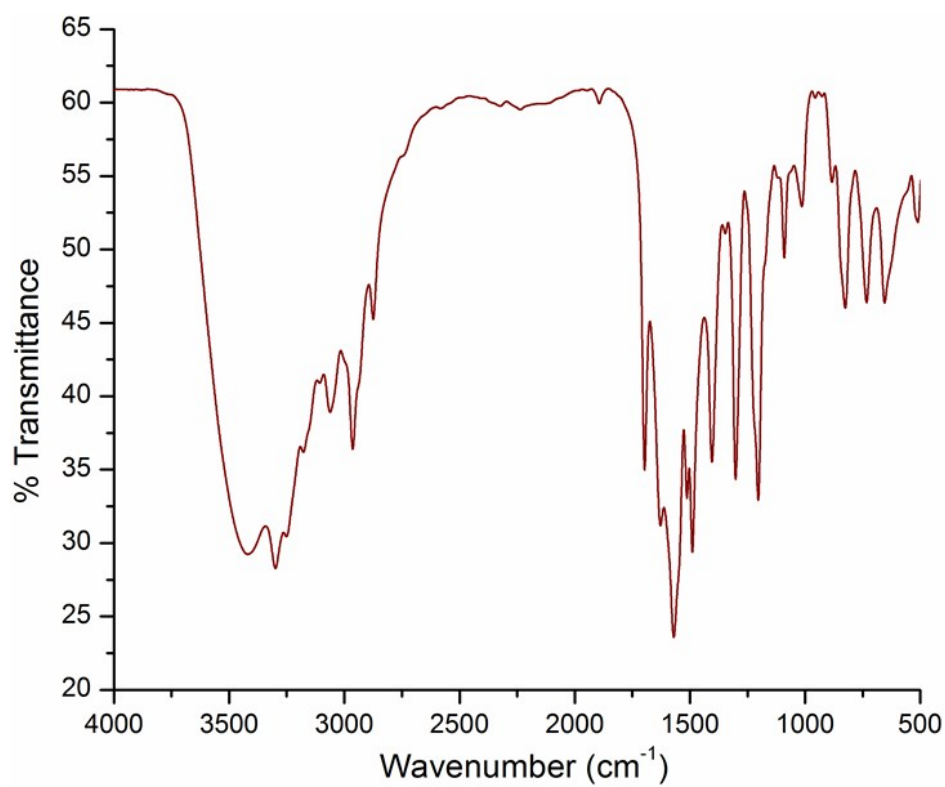


Figure S12: FT-IR spectrum of complex **1c** of **L₁** recorded in KBr pellet.

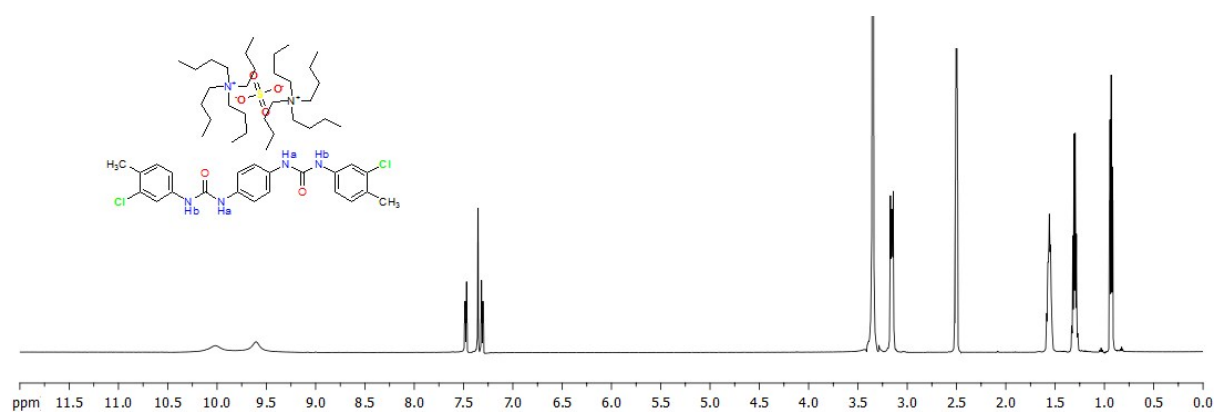


Figure S13: ^1H NMR full and expanded spectrum of divalent sulphate complex **1d** of **L₁** as recorded in $\text{DMSO-}d_6$ at 298 K.

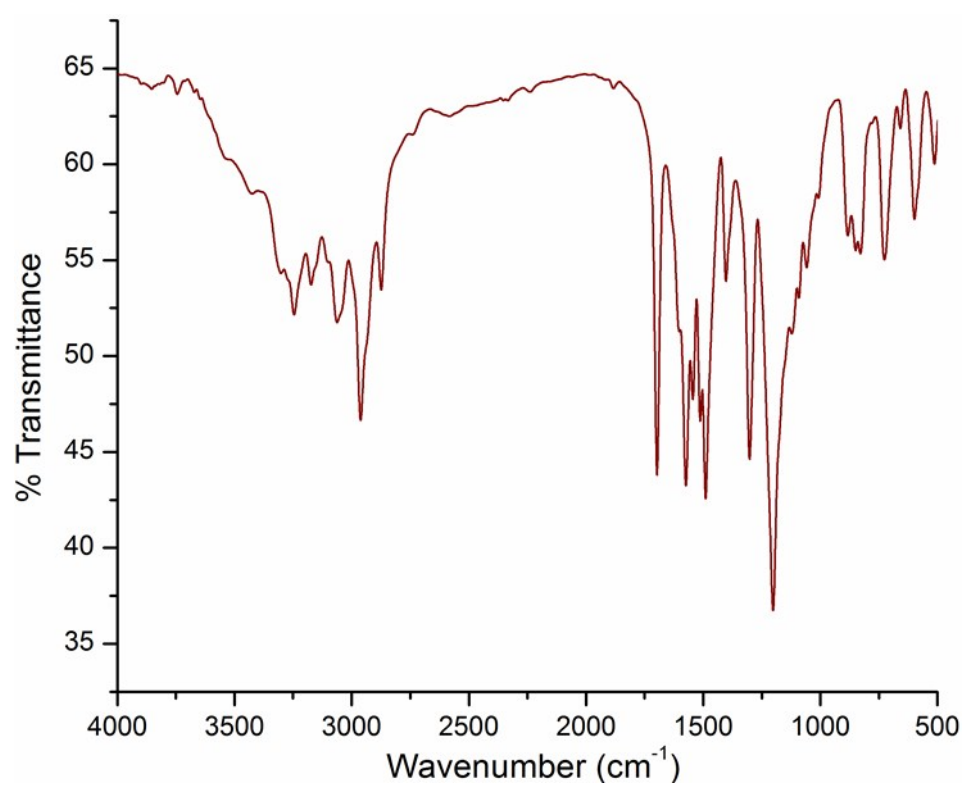


Figure S14: FT-IR spectrum of complex **1d** of **L₁** recorded in KBr pellet.

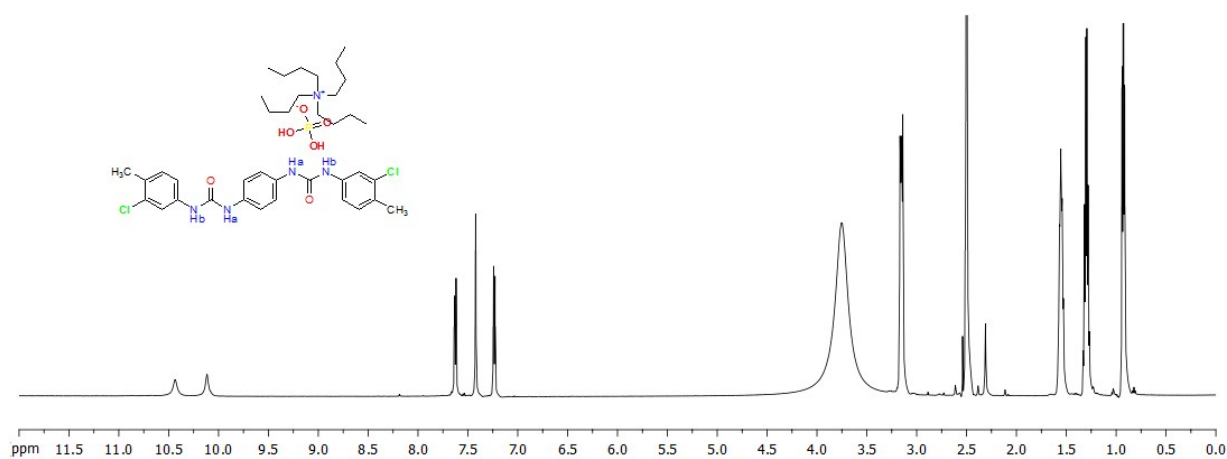


Figure S15: ^1H NMR full and expanded spectrum of dihydrogenphosphate polymer trapped complex **1e** of **L₁** as recorded in $\text{DMSO-}d_6$ at 298 K.

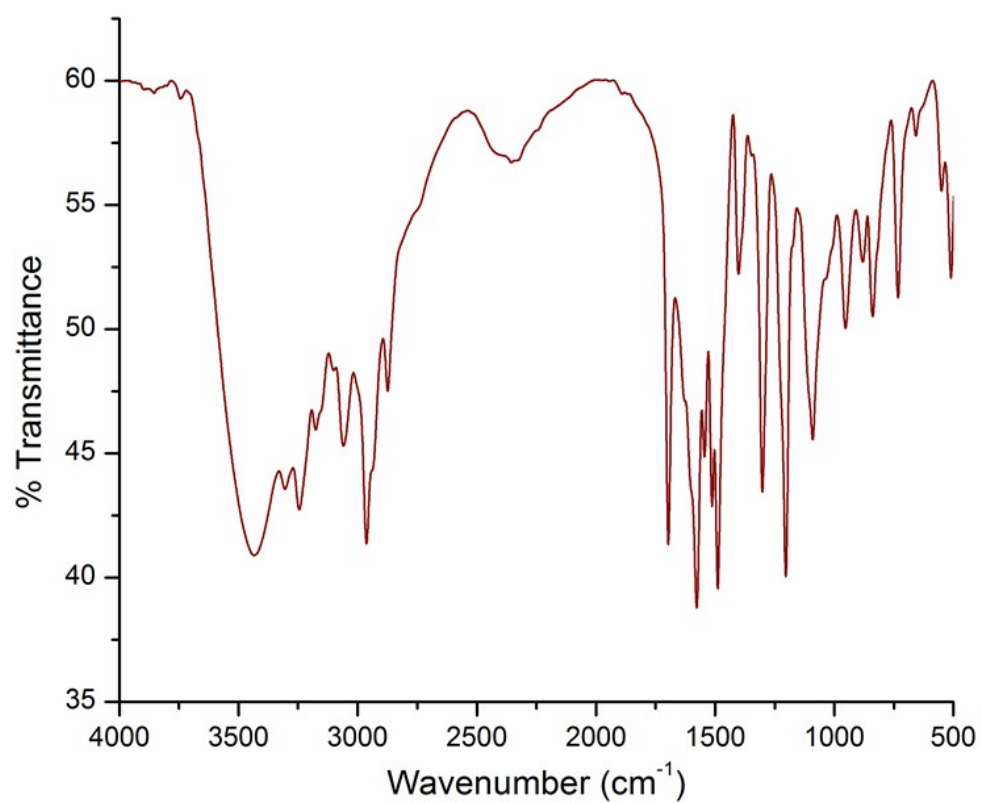


Figure S16: FT-IR spectrum of complex **1e** of **L₁** recorded in KBr pellet.

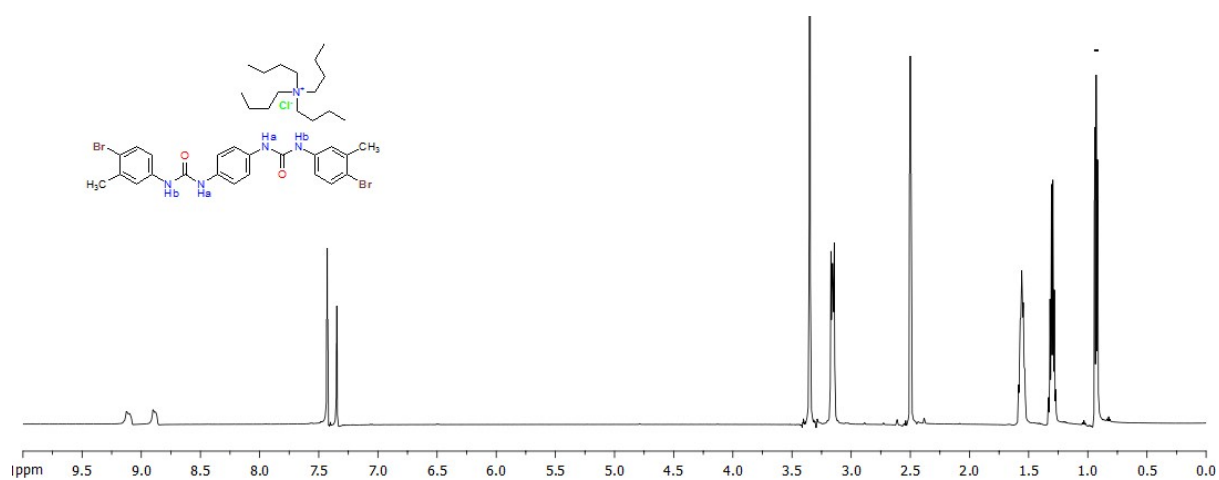


Figure S17: ^1H NMR full and expanded spectrum of chloride complex **2a** of **L₂** as recorded in $\text{DMSO-}d_6$ at 298 K.

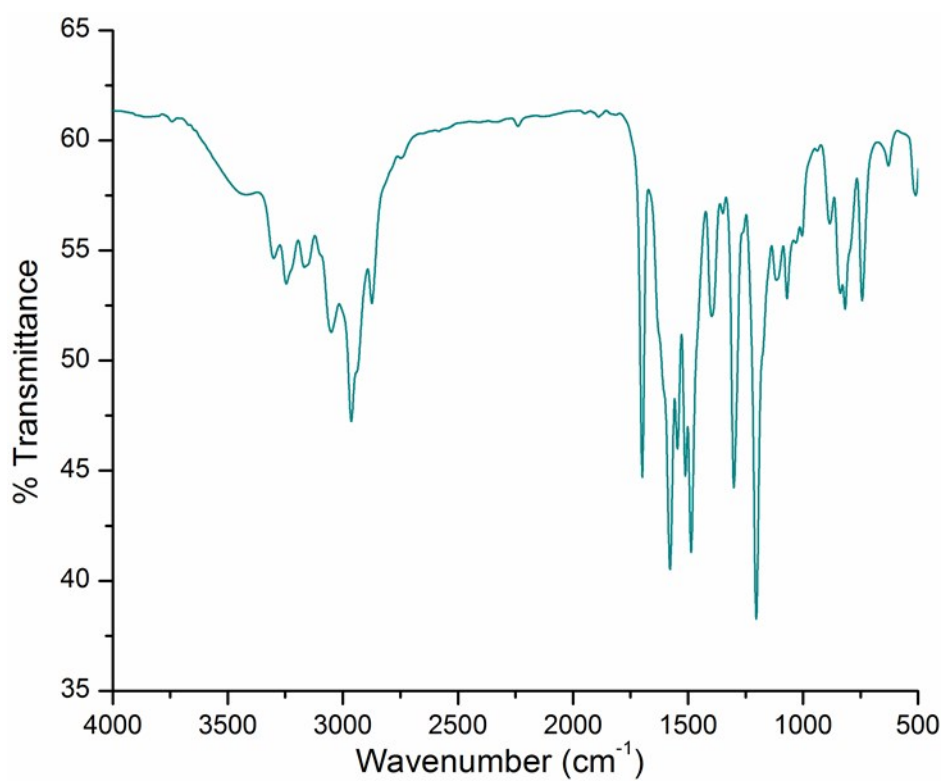


Figure S18: FT-IR spectrum hydrated-acetate complex **2a** of **L₂** recorded in KBr pellet.

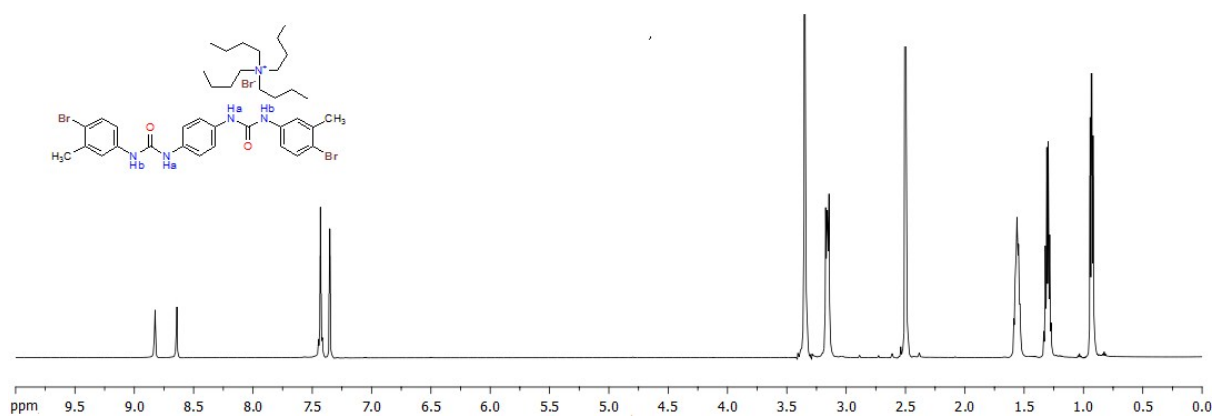


Figure S19: ¹H NMR full and expanded spectrum of bromide entrapped complex **2b** of **L₂** as recorded in DMSO-*d*₆ at 298 K.

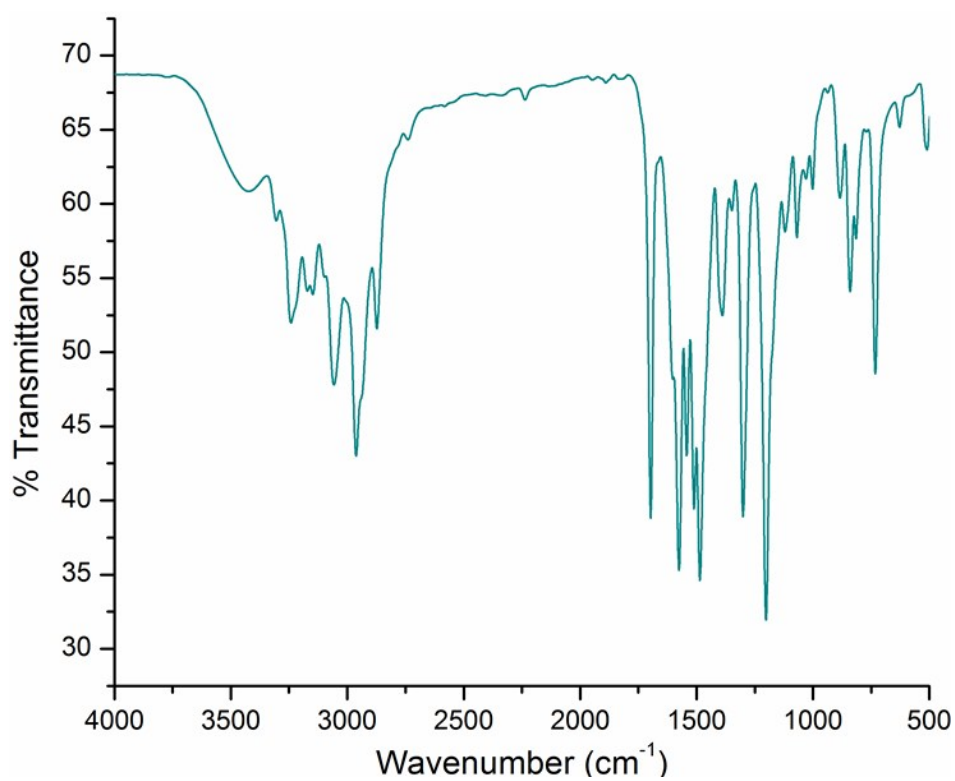


Figure S20: FT-IR spectrum of complex **2b** of **L₂** recorded in KBr pellet.

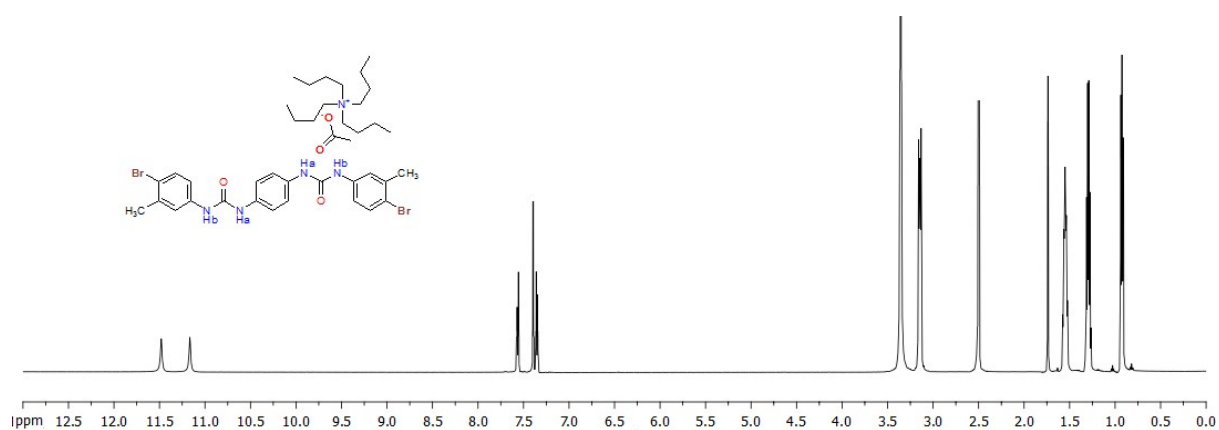


Figure S21: ^1H NMR full and expanded spectrum of acetate entrapped complex **2c** of **L₂** as recorded in $\text{DMSO-}d_6$ at 298 K.

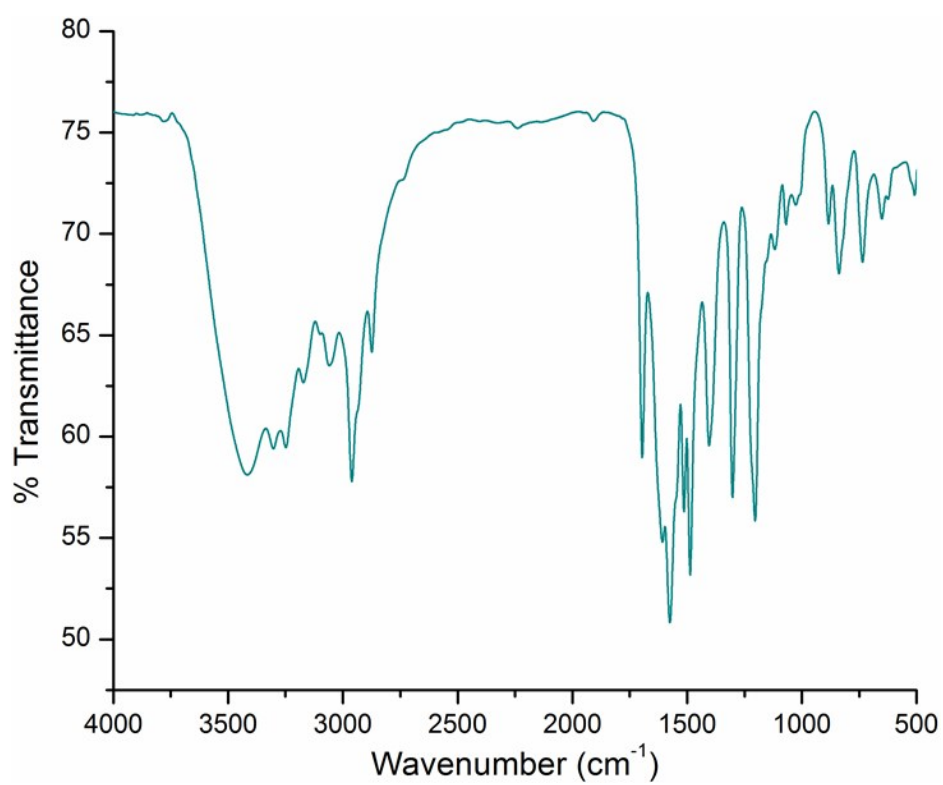


Figure S22: FT-IR spectrum of complex **2c** of **L₂** recorded in KBr pellet.

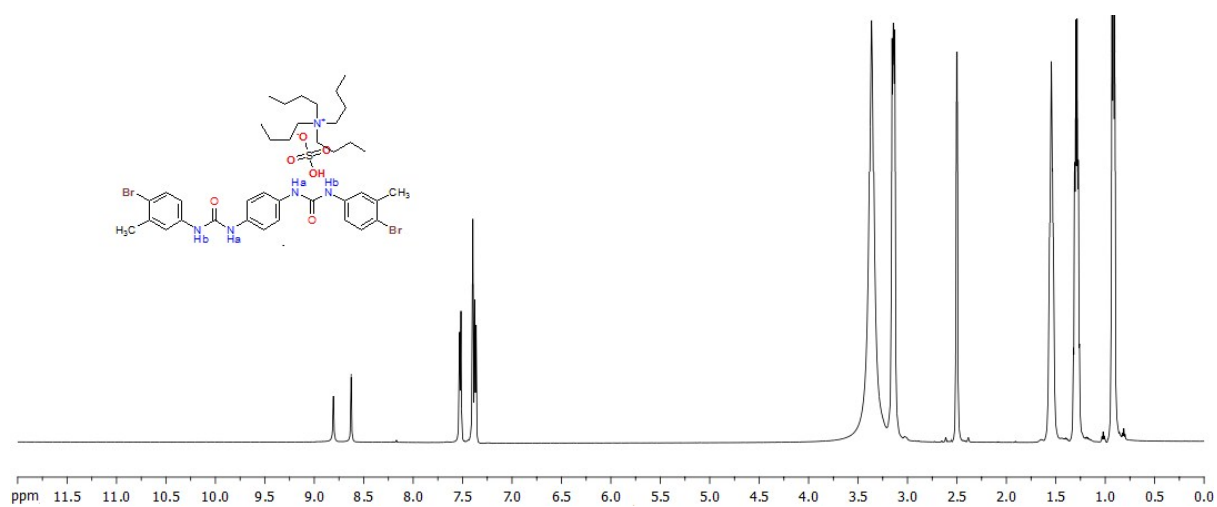


Figure S23: ^1H NMR full and expanded spectrum of hydrogensulphate dimer entrapped complex **2d** of **L₂** as recorded in $\text{DMSO-}d_6$ at 298 K.

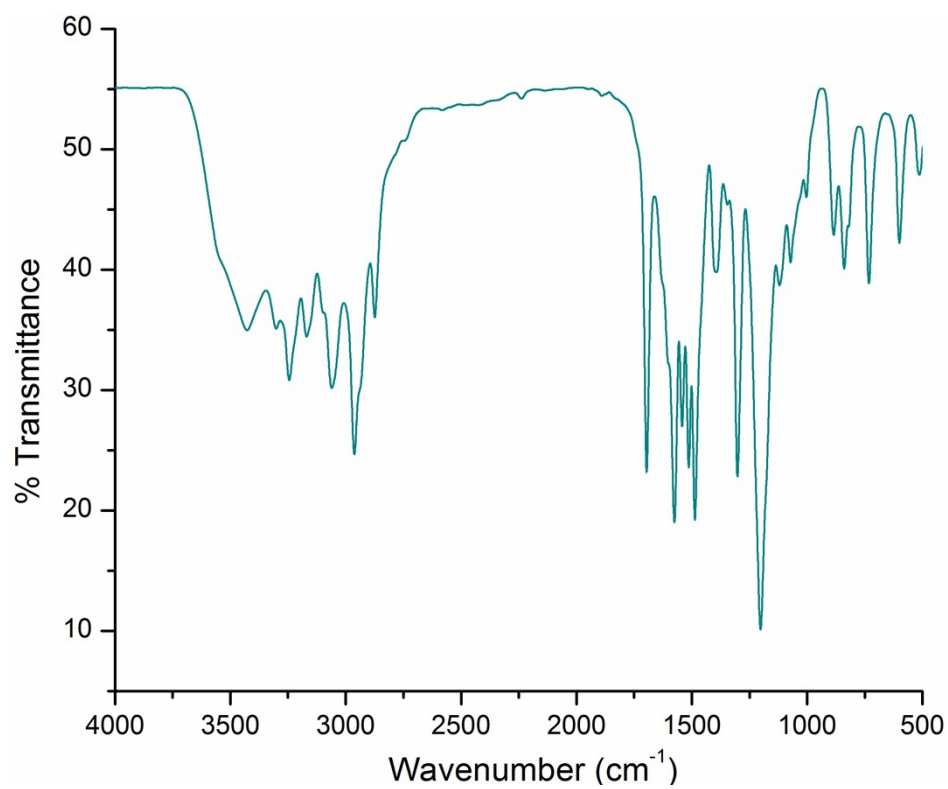


Figure S24: FT-IR spectrum of complex **2d** of **L₂** recorded in KBr pellet.

Table S1. Hydrogen bonding distances (Å) and Bond angles (°) in the neutral anion-receptor complexes:

Ligand/Complex	D–H···A	<i>d</i> (D···H)/Å	<i>d</i> (H···A)/Å	<i>d</i> (D···A)/Å	<D–H···A/°	Symmetry codes
1a	N1–H1N···Br1	0.86	2.52	3.351(5)	162	1/2-x,-1/2+y,1/2-z
	N2–H2N···Br1	0.86	2.50	3.332(4)	163	1/2-x,-1/2+y,1/2-z
1b	N1–H1N···O2	0.86	1.93	2.76(13)	164	x,y,z
	N2–H2N···O3	0.86	2.00	2.83(13)	165	x,y,z
	O4–H4O···O3	0.82	1.83	2.64(13)	169	1-x,1-y,-z
1c	N1–H1N···O3	0.86	2.00	2.834(4)	163	x,y,z
	N2–H2N···O4	0.86	1.93	2.776(4)	166	x,y,z
	N3–H3N···O5	0.86	1.97	2.785(4)	158	1-x,-1/2+y,1/2-z
	N4–H4N···O6	0.86	1.96	2.809(4)	167	1-x,-1/2+y,1/2-z
1d	N1–H1N···O4	0.86	2.00	2.833(7)	162	x,y,z
	N1–H1N···O6	0.86	2.06	2.854(7)	154	x,y,z
	N2–H2N···O4	0.86	2.58	3.248(6)	135	x,y,z
	N2–H2N···O5	0.86	2.17	2.927(6)	147	x,y,z
	N2–H2N···O3	0.86	1.95	2.765(5)	159	1-x,-y,1-z
	N3–H3N···O6	0.86	2.54	3.299(6)	148	1-x,1/2+y,1/2-z
	N3–H3N···O3	0.86	2.00	2.798(5)	154	x,1/2-y,-1/2+z
	N3–H3N···O4	0.86	2.29	3.051(6)	148	x,1/2-y,-1/2+z
	N3–H3N···O5	0.86	2.51	3.233(6)	142	x,1/2-y,-1/2+z
	N4–H4N···O6	0.86	2.03	2.828(6)	153	1-x,1/2+y,1/2-z
	N4–H4N···O5	0.86	2.00	2.835(6)	163	x,1/2-y,-1/2+z
1e	N1–H1N···O5	0.86	2.13	2.923(4)	153	x,y,z
	N2–H2N···O4	0.86	2.01	2.833(4)	161	x,y,z
	O2–H2O···O5	0.82	1.75	2.549(4)	164	1-x,-y,1-z
	O3–H3O···O4	0.82	1.76	2.558(4)	166	-x,-y,1-z
2a	N1–H1N···Cl1	0.86	2.35	3.181(6)	161	3/2-x,1/2+y,1/2-z
	N2–H2N···Cl1	0.86	2.35	3.181(6)	162	3/2-x,1/2+y,1/2-z
2b	N1–H1N···Br2	0.86	2.52	3.352(6)	163	1/2-x,-1/2+y,1/2-z
	N2–H2N···Br2	0.86	2.49	3.319(6)	163	1/2-x,-1/2+y,1/2-z
2c	N1–H1N···O3	0.86	1.97	2.809(7)	164	x,y,z
	N2–H2N···O4	0.86	1.92	2.766(7)	166	x,y,z
	N3–H3N···O6	0.86	1.96	2.778(7)	158	1+x,y,z
	N4–H4N···O5	0.86	1.97	2.812(7)	166	1+x,y,z
2d	N1–H1N···O10	0.86	2.04	2.902(7)	175	x,y,z
	N2–H2N···O11	0.86	2.15	2.992(7)	166	x,y,z
	O8–H8···O11	0.82	1.83	2.646(6)	172	1-x,1-y,1-z

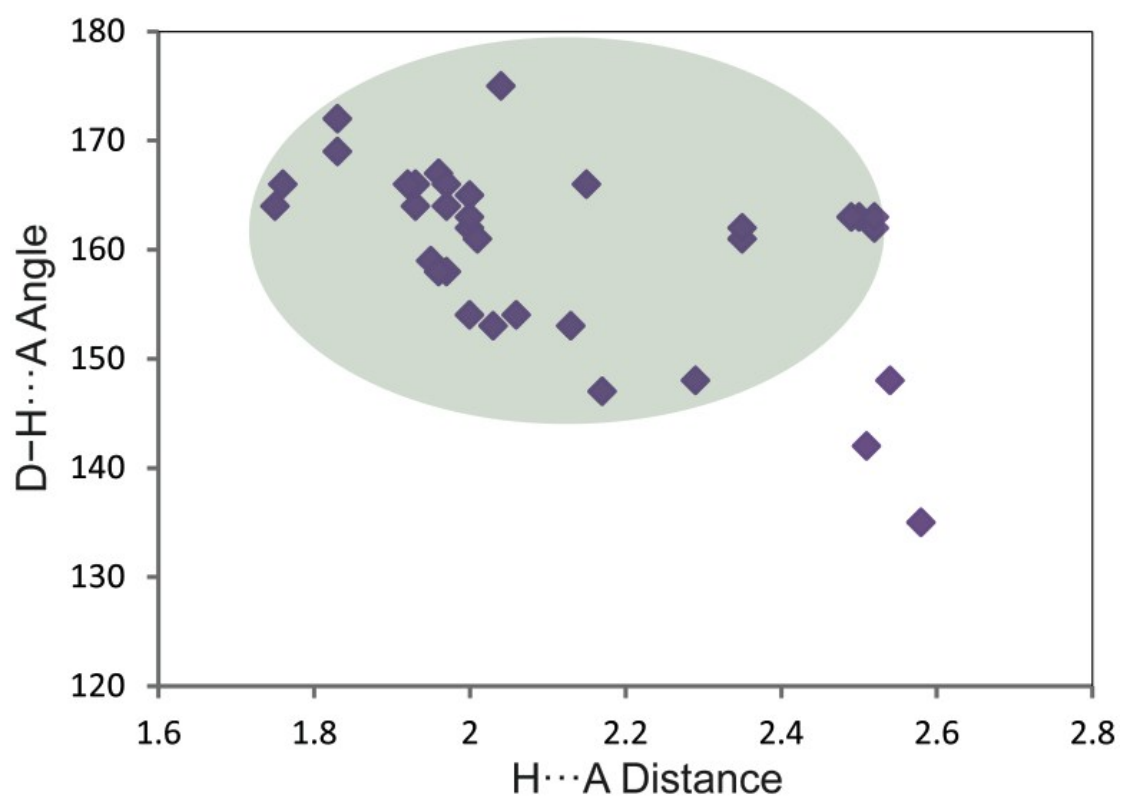


Figure S25. The scatter plot of D–H···A angles vs. H···A distances of the hydrogen bonds in neutral halide and oxyanion complexes **1a–1e**, **2a–2d** of receptors **L₁** and **L₂** and encircled area in the plot representing most of the interactions are present in strong hydrogen-bonding regions.